A Simplified Elastoplastic Method for the Calculation of LMFR Pipework Submitted to Monotonous Loadings

M. N. Berton, C. Aillaud, Ph. Martin
CEA-CEN Cadarache, St. Paul-lez-Durance, France
D. Gamby
ENSMA, Poitiers, France

ABSTRACT

The main characteristics and the basic assumptions of a simplified elastoplastic pipework calculation method are described.
This is a low cost method of obtaining the overall displacements of a line. It is well adapted to thin flexible pipes subjected to high thermal loadings with low internal pressure.
The treatment of monotonous loadings (i.e. producing locally monotonous stresses and strains) is already operational, and some checks for this special case are included.

1. PURPOSE

The choice of an elastoplactic pipework calculation method is closely related to the problem of the calculation cost, which depends mainly on the dimensions of this type of component.
The conventional beam theory based on the assumption that plane sections remain plane is less suitable for calculations on very thin and flexible LMFR type piping subject to larger thermal loadings than for others.
Many methods have been explored and many calculation programs have been developed (ref. 1), varying from shell theory to beam theory, including a number of intermediate variants and local or global plasticity procedures.
The VICTUS tests -sodium thermal shock tests on piping- and the calculations which have been carried out in parallel (ref. 2, 3, 4, and 5) pointed out the advantages and disadvantages of the various methods and made it possible to define objectives for a simplified electoplastic piping calculation method which can be used at the project level.
The intention was therefore to develop a calculation method suitable for LMFR type pipework (thin and flexible).

- Inexpensive and simple to use.
- Applicable in the range close to the yield point.
- Which allow correct evaluation of overall deformations in a pipeline.
- Taking temperature variations across the thickness (due to thermal shocks) into consideration.
- Which can be included in one of the CASTEM (TEDEL) (ref. 6) system programs, i.e. in a well-determined plasticity processing method.

This type of method will not directly give local deformations and stresses. If necessary, these can be estimated by local calculations for which the boundary conditions will be supplied by this global calculation procedure.
To satisfy these requirements, the following options were selected :
The basic calculation uses a beam finite element model which allows the manipulation of conventional generalized variables to which new generalized variables related to deformation of plane sections (ovalization) and thermal gradient across the thickness are added.
Obviously, the variables related to ovalization are not independent : these are internal variables.
The search for potentials necessary for processing plasticity on the global variables leads to the use of analytic calculations using the shell theory.
This method can therefore be defined as a combined "beam" finite element - "shell" analytic method (for more details, see ref. 12).

2. NOTATIONS

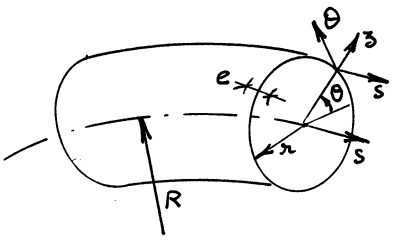

$I = \pi r^3 e$ Inertia moment of cross section
$J = 2I$ Polar inertia moment of cross section
$f = eR/r^2$ Elbows characteristic parameter
E Young Modulus
ν Poisson ratio
α Thermal expansion coefficient
σ_E Yield stress

The parameters σ are stresses, ε and γ deformations, $\mathcal{M}$ and M moments, ρ curvatures.
Dimensionless parameters m refer to reduced moments and λ to reduced curvatures.
Subscript f designates bending loads, o ovalization loads, t torsion loads, E designates initiation of plasticity.
ΔT is the linear thermal load across the thickness.

3. BASIC ASSUMPTIONS

3.1 Two generalized variables related to the ovalization phenomenon - M_o and ρ_o - are used in addition to the moment - M_f (bending) and M_t (torsion) and associated curvatures- ρ_f and ρ_t which are the generalized variables classically used in beam type methods. These are internal variables since they depend on bending variables.
$\rho_o = 3O/r$ (O ovalization) is the 2θ -term amplitude of the local curvature and M_o is (except for a multiplying coefficient) the 2θ -term amplitude of the local bending moment.
In the elastic range :

$$M_o = \frac{E}{12(1-\nu^2)} \pi r e^3 \left(1 + \frac{1}{12 f^2}\right) \rho_o = D\rho_o$$

3.2 The relation between ovalization moment and bending moments in elbows is the same in the plastic range as in the elastic one.
From the ovalization propagation theory (ref. 7), reference 8 formulates the ovalization of an angle ψ-elbow and its adjacent straight parts, subjected to an arbitrary moment :

$$O(s) = \mu O_\infty / 2 \int_{-R\psi/2}^{R\psi/2} M_f(y) e^{-\mu|s-y|} \left((1+\beta)\cos\mu|s-y| + (1-\beta)\sin\mu|s-y|\right) dy \quad (1)$$

where $\mu = \sqrt{\frac{e}{r^3}\sqrt{3}}$ **ovalization attenuation parameter**

O_∞ **ovalization of an infinite elbow under a unit bending moment**

$$\beta = \frac{e}{r}\sqrt{3\left(1 + \frac{1}{12 f^2}\right)} \frac{1}{1-\nu}$$

In the elastic range, linearity between ovalization moment and ovalization ($M_o = D\rho_o = D3O/r$) leads to a relation $M_o = G(M_f)$ (2) . We will make the simplifying assumption that this equation (2) is applicable in the plastic range. It is good for low plastic strains and could be modified if it is shown to be necessary in the debugging stage.

3.3 The relation between flexibility and ovalization is identical in the plastic range and in the elastic one. The additional flexibility in elbows depends on ovalization by the linear relation $\frac{d\varphi}{ds} = \frac{3O}{4R}$ (ref. 8) which leads to the ASME flexibility coefficient :

$$k = 1 + \frac{3EI}{4R} \frac{O(s)}{M_f(s)} \quad (3)$$

3.4 - In a section, plastic flow corresponding to each generalized strain can be described by differential systems involving the generalized contributing forces coupled together.

- The implements of the various generalized forces do not all have the same effect in producing a plastic increment to a given generalized strain : some contributions can be neglected.
- We will therefore write as many systems as there are generalized strains (in our case 3).
- In the case of monotonous loadings dealt with here, taking account of the preceeding comments, the above-described systems can be reduced to the form of moment-curvature relations :

$$\begin{aligned} f_1(M_f, M_t, \Delta T, \rho_f) &= 0 \\ f_2(M_o, M_t, \Delta T, \rho_o) &= 0 \\ f_3(M_t, \Delta T, \rho_t) &= 0 \end{aligned} \quad (4)$$

Note that coupling between bending and ovalization is not included since it will be treated out of the section according to assumption 3.1 and 3.3.
Each of these equations can be represented by a curve $M_i(\rho_i)$, including a linear part followed by a non-linear part showing even for the case of elastic-perfectly plastic material an apparent hardening, and affected by the other forces M_j coupled to M_i.

4. PLASTICITY SOLUTION DIAGRAM

This method has been incorporated into TEDEL, a beam finite element program in the CASTEM system (ref. 6), and work was required in three areas :

(a) Complete revision of internal iterations (section plasticity) which will be replaced by 3 solutions used to calculate generalized strains and stresses.
(b) Adding new ovalization variables in the generalized stress calculations.
(c) Including the flexibility due to ovalization in external iterations (structure reequilibrium) by including the corresponding plastic reequilibrium forces.

5. PLASTICITY IN A SECTION UNDER MONOTONOUS LOADING (determination of f_1, f_2 & f_3)

These results are only applicable for loads producing locally monotonic strains, i.e. satisfying Ilyushin's simple loading theorem. In the case of a radial thermal loading combined with another loading (flexion, ovalization or torsion) this hypothesis requires the two must be proportional. The loading path in stress or strain spaces will therefore be very particular. The calculations described here are obtained by punctual and simultaneous application of all loads (i.e. like an elastic calculation) and are equivalent to proportional increasing loadings.

In the case of bending (f_1) and ovalization (f_2), these results are strictly identical to those obtained for a locally monotonous load. Under torsion (f_3), for which the calculation is not unidirectional (see section 5.1.3), a comparison with shell-finite element calculations shows very little difference between the proposed formulation and the monotonous load case calculation.

Some simplifying assumptions have been made in carrying out these analytic calculations ; these will be specified for each case dealt with.

Finally, the use of dimensionless parameters allows expressing functions f_1, f_2 and f_3 in a form which does not include the geometric and in case of perfect plasticity material properties of the pipe.

5.1 Simplified calculations based on shell theory and perfect plasticity

5.1.1 Bending loads (function f_1)

Calculation assumptions

H1 conventional thin shell theory assumptions
H2 perfect plastic material with elastic limit σ_E
H3 linear thermal loading through the thickness ΔT
H4 pipe bending : the axial strains are constant across the thickness and vary with $\sin\theta$ around the section
H5 the stress state is unidirectional along the pipe axis to allow a simple analytic solution (which is equivalent to only considering the axial effect of ΔT).

The bending moment across the section is given by :

$$M_f = \int_0^{2\pi} \int_{-e/2}^{e/2} \sigma_s(z,\theta)\, r \sin\theta \, r\, dz\, d\theta \qquad (5)$$

where $\varepsilon_s(z,\theta) = \rho_f r \sin\theta - \alpha \Delta T z/e$

Dimensionless variables

- Reduced curvature $\lambda_f = \rho_f / \rho_{Ef}$ $\qquad \rho_{Ef} = \sigma_E / E r$
- Reduced moment $m_f = M_f / M_{fp}$ $\qquad M_{fp} = 4 \sigma_E e r^2$
- Thermal pseudo curvature $k_T = E \alpha \Delta T / 2 \sigma_E$

Depending on the values of k_T and λ_f which determine the various cases for the distribution of plastic zones in the section, the integration calculation (5) leads to curves f_1 plotted in fig. 1.

5.1.2 Ovalization load (function f_2) ; ref. 11

Calculation assumptions : assumptions H1, H2, H3 above apply, together with :

H6 pipe ovalization : tangential strains vary linearly through the thickness and with $\cos 2\theta$ around the circumference $\varepsilon_\theta(z,\theta) = \rho_0 z \cos 2\theta = z\, \rho(\theta)$
H7 plane stress assumption in the axial direction ($\sigma_z = 0$)

The local bending moment is obtained by integrating across the thickness :

$$m(\theta) = \int_{-e/2}^{e/2} z\, \sigma_\theta(z,\theta)\, dz \qquad (6)$$

Dimensionless variables

- Local reduced curvature $\lambda(\theta) = \rho(\theta) / \rho_E$ $\qquad \rho_E = 2 \sigma_E / Ee$
- Reduced local moment $m(\theta) = m(\theta) / m_p$ $\qquad m_p = \sigma_E e^2/4$

Ovalization moment : this will be defined as the second order term of the Fourier series expansion of the local bending moment :

$$m_0 = \frac{1}{\pi} \int_{-\pi}^{\pi} m(\theta) \cos 2\theta \, d\theta \qquad (8)$$

In the case of ovalization with radial thermal load, the curvature becomes : $\rho(\theta) = \rho_0 \cos 2\theta - \alpha \Delta T/e$ where ρ_0 is the ovalization curvature $\rho_0 = 3O/r$, or, expressed in dimensionless variables :

$$\lambda(\theta) = \lambda_0 \cos 2\theta - k_T \qquad (9) \qquad \lambda_0 = \rho_0 / \rho_E \qquad k_T = E\alpha\Delta T / 2\sigma_E$$

The integration calculation (8) with $m(\theta)$ given by (6) and $\lambda(\theta)$ by (9) gives the following, depending on the values of k_T and λ_0 which determine the various cases of plastic zone distribution in the section gives curves f_2 plotted in figure 3.

5.1.3 Torsion loading (function f_3)

. Calculation assumptions : assumptions H1, H2 and H3 above apply together with the following :

H8 : torsion shear strain γ is assumed to be constant circumferentially and through the thickness.

H9 : an additional assumption is made about the stress distributions in the plastic zone (see below)

. The torsion moment is obtained by integration :

$$M_t = \int_0^{2\pi} \int_{-e/2}^{e/2} \tau(z)\, r^2 dz d\vartheta = 2\pi r^2 \int_{-e/2}^{e/2} \tau(z)\, dz \qquad (10)$$

. Shear stress calculation ($\tau(z)$)

- In the elastic range $\tau(z) = \rho_t G r \sqrt{3}$ $\qquad G = E/2(1+\nu)$
- In the plastic range $\tau(z)$ can be calculated by solving the system :

* Von Mises plasticity criterion : $\sigma_* = \sigma_E$

* Normality rule : Subscript p designate plastic part of strain :

$$\{d\varepsilon^p\} = \left\{\frac{\partial \sigma_*}{\partial \sigma}\right\} d\varepsilon^*$$

* Total strains definition : $\gamma = \rho_t r$

$$\varepsilon_z(z) = \varepsilon_\theta(z) = 2z/e \times \alpha \Delta T/2$$

which permit to calculate plastic strains.

For proportional applied loads, strain increments can be replaced by strains.

When the following dimensionless variables are defined :

$$\lambda_t = \rho_t / \rho_{Et} \qquad \rho_{Et} = \sigma_E / G r \sqrt{3} \qquad k'_T = E\alpha\Delta T / 2\sigma_E (1-\nu)$$

The system reduces to a 4th degree equation in $\tau(z)$. By making approximations to this solution, the following is obtained (assumption H9) :

$$\tau(z) = \frac{\sigma_E}{\sqrt{3}\, Ch \frac{C k'_T}{C + \lambda_t - 1} \frac{2}{e} z} \qquad \text{where} \qquad C = 3\frac{1-\nu}{1+\nu} \qquad (11)$$

. Calculation of the integral (10) leads to calculate the reduced torsion moment :

$$m_t = M_t / M_{tp} \qquad M_{tp} = M_{te} = \sigma_E J / r\sqrt{3}$$

depending on the values of λ_T and k'_T, we obtain curves plotted in figure 5.

5.1.4 Influence of torsion on the f_1 (bending) and f_2 (ovalization) funtions

A simplified formulation involving a reduction of the yield stress σ_E is proposed to take account of this effect.

The Von Mises plasticity stress is $\sigma_* = \sigma_E$ gives :

$$\sigma_z^2(z,\vartheta) + \sigma_\theta^2(z,\vartheta) - \sigma_z(z,\vartheta)\sigma_\theta(z,\vartheta) = \sigma_E^2 (1 - 3\tau^2(z)/\sigma_E^2) \qquad (12)$$

in which the reduced distorsion moment is the integral over the sections.

$$m_t = \frac{1}{S} \iint_S \frac{\sqrt{3}\,\tau(z)}{\sigma_E} dS$$

The mean value of the second term of equation (12) over the section will be : $\sigma'^2_E = \sigma_E^2 (1 - m_t^2)$

The yield stress will therefore be replaced by $\sigma'_E = \sigma_E \sqrt{1 - m_t^2}$

5.2 Application to plasticity with hardening

In the case of a plastic with hardening material, a monotonic load can be processed by the superposition of perfectly plastic materials.

5.3 Checking expressions of f_1, f_2 and f_3

The family of curves f_1, f_2, f_3 have been compared with calculations carried out using the CASTEM INCA program (ref. 6) using thin shell elements with plasticity integration points in the thickness.

- Bending (f_1) : mesh of a half section of the pipework (24 shell elements). By using the generalized plane deformation option (ref. 10), a beam type bending moment can be imposed. Two calculations were carried out :

Figure 1 : with the axial effect of ΔT only, the proposed f_1 function is obtained exactly.

Figure 2 : with the radial and tangential effects of ΔT, the result is different for high values of plastic strain.

- Ovalization (f_2) : mesh of one quarter of the section (24 shell elements). Two calculations were carried out.

Figure 3 : a plane stress calculation (influence of the radial effect of ΔT), gives the proposed function.

Figure 4 : a plane strain calculation (influence of the tangential and axial effects of ΔT), results are different for high values of plasticity.

- Torsion (f_3) : mesh of one section of axisymmetric pipe (one shell element). The torsion load is applied by a tangential load in mode 0. The tangential and radial effects of ΔT are taken into account.

Figure 5 : a comparison with f_3 is quite satisfactory.

Comments : the calculations taking account of tangential and radial effects of ΔT (figures 2 - 4 - 5) are physically more correct. Adjustments taking account of the Poisson's ratio and the bi-

directional nature of the plastic flow can be carried out of the f_1 and f_2 functions, but this is only really necessary for high values of ΔT.

6. CALCULATIONS FOR VICTUS TESTS

The first phase in VICTUS loop 1 and 2 tests (fig. 6) consisted of a thermal shock superimposed on a constant primary load which in itself did not lead to plastic strains (ref. 2 and 4).
These tests can be broken down into an elastic load, a monotonic plastification during the shock and an elastic unloading phase, and can be calculated in this manner using the simplified method.
The following residual cold displacements and strains :

- measured,
- calculated by the simplified method,
- calculated by a shell-finite element program (BILBO ref. 6),
- calculated by a beam-finite element program with special elements in the elbow (TEDEL ref. 6),

are compared in the following tables.

Expansion loop 1 : primary in-plane bending load

	Residual displacement at end of loop in mm	Mean residual ovalization of elbows
Test	6.5	$.9\ 10^{-3}$
Simplified method	7.1	$1.8\ 10^{-3}$
BILBO	10.3	$1.75\ 10^{-3}$
TEDEL	14.2	-

Expansion loop 2 : primary out-of-plane bending load and torsion

	Residual displacement at top of loop in mm	Residual ovalization of bottom elbows	Torsion of the bottom straight part in rd/mm
Test	6.5	$1.4\ 10^{-3}$	-
Simplified method	6.2	$1.7\ 10^{-3}$	$.\ 38\ 10^{-6}$
BILBO	7.0	$1.7\ 10^{-3}$	$.\ 32\ 10^{-6}$
TEDEL	8.5	$2.8\ 10^{-3}$	0

These results demonstrate firstly the high scatter of results given by the various calculation methods for thermal shock case, and secondly the very respectable performance of the simplified method.

7. CONCLUSIONS

The first result obtained using this simplified method are quite promising. Other checks are being carried out. Some improvements on points described within the presentation are expected.
Work will continue to allow processing non-monotonic loads.

REFERENCES

1. Developments in methods of inelastic piping systems. Pipework design and operation. IM ech E conference publication 1985-1 - C18/85. J.T. BOYLE - J. SPENCE.
2. Thermal shocks experiments in piping system
   M.N. BERTON - J.L. CARBONNIER - P. PERMEZEL. E 6/4 SMIRT 8 1985.
3. Piping system inelastic calculation during thermal shocks. Comparison with experiments.
   M.N. BERTON - P. PERMEZEL. E 6/5 SMIRT 8 1985
4. Thermal shock experiments and inelastic calculations in piping system.
   M.N. BERTON - H.G. FAILLA - P. PERMEZEL. E2/3 SMIRT 9 1987
5. Thermal shock experiments and inelastic calculations in piping system.
   M.N. BERTON - H.G. FAILLA - Ph. MARTIN - P. PERMEZEL. SMIRT 10 1989
6. "CASTEM (CEA SEMT)"
   A system of finite elements computer programs. Porto Alegre Brazil 1978. Proc. Conf. Struct. Analysis, Design and Const. Nucl. Power Plant Paper 40. A. HOFFMANN - A. COMBESCURE
7. Propagation of ovalization along straight pipes and elbows.
   A. MILLAUD - R. ROCHE. M 10/1 SMIRT 6 1981
8. An accurate method for calculation of stress intensification factors in elbows. B7/2 SMIRT 8 1985.
   M.N. BERTON - P. BAILLAGOU - J.L. CARBONNIER

9. Strategies for non linear static calculations.
A. COMBESCURE. ISPRA courses Sept. 4-5th, 1986
10. Generalized plane strains : an interesting and efficient extension of the standard plane stress and plane strain analysis.
A. COMBESCURE. B 8/8 SMIRT 8 1985
11. Effect of a radial thermal gradient on the ovalization of a pipe section.
C. AILLAUD - M.N. BERTON - D. GAMBY
Int. Jour. of Pressure Vessel and Piping. Vol. 37. March 89.
12. Elaboration et validation d'une méthode de calcul élastique et inélastique de tuyauterie, basée sur une modélisation en poutre et prenant en compte le chargement thermique dans la paroi. Doctoral thesis of C. AILLAUD. To be defended in June 89. CEA - University of Poitiers.

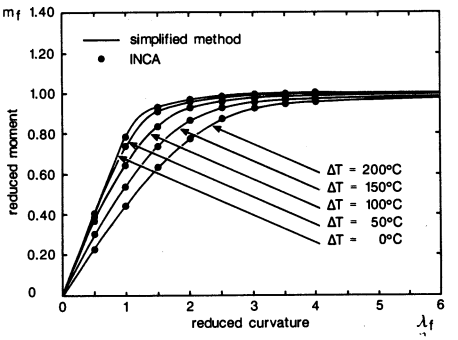

Figure 1 : BENDING OF A PIPE SECTION
INFLUENCE OF ΔT . FUNCTION F1
INCA CALCULATION WITH THE AXIAL EFFECT OF ΔT

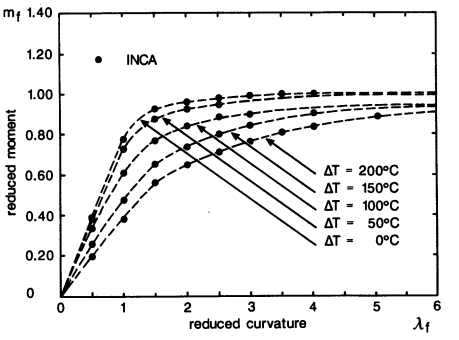

Figure 2 : BENDING OF A PIPE SECTION . INFLUENCE OF ΔT
INCA CALCULATION WITH THE TANGENTIAL
AND AXIAL EFFECTS OF ΔT

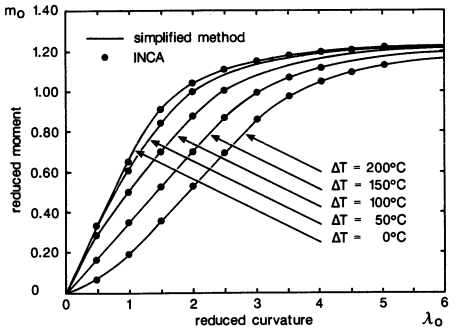

Figure 3 : OVALIZATION OF A PIPE SECTION
INFLUENCE OF ΔT . FUNCTION F2
INCA PLANE STRESS CALCULATION

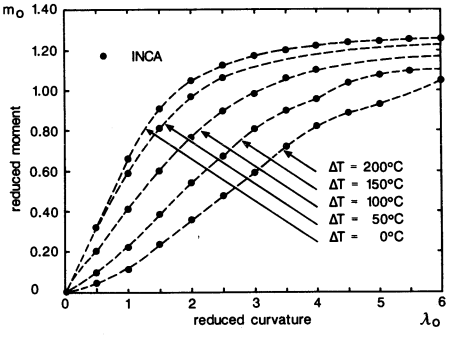

Figure 4 : OVALIZATION OF A PIPE SECTION
INFLUENCE OF ΔT
INCA PLANE STRAIN CALCULATION

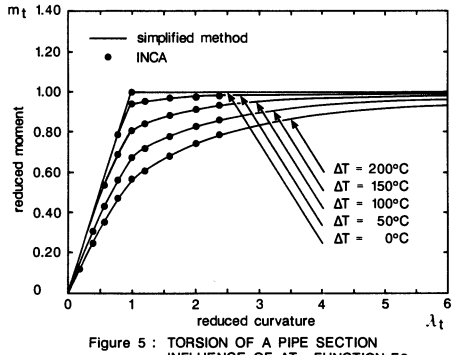

Figure 5 : TORSION OF A PIPE SECTION
INFLUENCE OF ΔT . FUNCTION F3
INCA CALCULATION

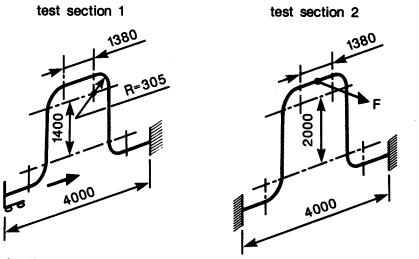

pipes dimensions : (316 L)
diameter Ø = 219.18 mm
thickness e = 8.18 mm
bend's radius R = 305 mm

Figure 6 : THERMAL SHOCK VICTUS TESTS